Journal of the Optical Society of Korea
Vol. 20, No. 4, August 2016, pp. 470-475

ISSN: 1226-4776(Print) / ISSN: 2093-6885(Online)
DOI: http://dx.doi.org/10.3807/JOSK.2016.20.4.470

Effect of Filter Parameters on a Supercontinuum-Based All-Optical Tunable Thresholder

Huatao Zhu[1], Rong Wang[1], Tao Pu[1]*, Tao Fang[1], Peng Xiang[1], and Huihui Zhu[2]

[1]*Optoectronical Research Center, College of Communications Engineering, PLA University of Science and Technology, Nanjing 210007, China*
[2]*College of Automobile and Traffic Engineering, Guilin University of Aerospace Technology, Guilin 541004, China*

(Received April 5, 2016 : revised July 8, 2016 : accepted July 11, 2016)

In this paper, the effects of filter parameters on a supercontinuum-based all-optical thresholder are experimentally investigated. By tuning the filter parameters, the power transfer function and power transmission function are tailored. The experimental results show that a thresholder with short center wavelength has a better power function, and the slope in the middle level of the thresholder increases with increasing bandwidth. Through tuning the filter parameters, the thresholder can achieve a steplike power transfer function for optical thresholding, and a steplike power transmission function for optical self-switching. This makes the supercontinuum-based thresholder more flexible, and allows customization of performance to meet different demands in various applications.

Keywords : Ultrafast nonlinear processes, Fiber nonlinear optics, Threshold logic device
OCIS codes : (060.0060) Fiber optics and optical communications; (060.4510) Optical communications

I. INTRODUCTION

All-optical signal processing is an important enabling technology in optical communications systems. A thresholder based on simple and effective all-optical devices can work beyond the limits of electronics. The main function of an all-optical thresholder (AOT) is thresholding, which can suppress signals in the optical domain above or below a certain threshold. An ideal thresholding function is expected to have a step function for power transfer, and can be used in all-optical logic circuits [1] and analog-to-digital conversion [2]. AOTs based on a nonlinear-optical loop mirror (NOLM) [3-5] and nonlinear polarization rotation (NPR) [6] have been proposed for this application. A super-continuum [7] -based AOT has been proposed for optical self-switching, where a step power transmission function is required [8, 9]. We should note that the *power transfer function* is defined as the function of output power versus input power, while the *power transmission function* is the function of output-to-input-power ratio versus input power. Optical self-switching can be used to suppress multiple-access interference noise in an optical code-division multiple-access system [8, 9], and in optical regeneration [7, 10]. The supercontinuum-based AOT has a simple structure and is insensitive to polarization. In the existing literature, most proposed supercontinuum-based AOTs are composed of a fixed optical amplifier and optical filter for a certain optical communication system.

In this paper, the effects of filter parameters on a supercontinuum-based AOT are experimentally investigated. While tuning the input power of the signal injected into the highly nonlinear fiber (HNLF), the broadened spectrum is measured. The power transfer and transmission functions are tailored through tuning the optical filter, and investigated with different filter parameters. The experimental results show that the supercontinuum-based AOT can be used simultaneously for optical thresholding and self-switching. In addition, the AOT's performance in suppressing intensity noise is also investigated.

*Corresponding author: nj_putao@163.com
Color versions of one or more of the figures in this paper are available online.

II. OPERATING PRINCIPLE AND EXPERIMENTAL SETUP

The main processed approaches of a supercontinuum-based tunable AOT are intensity-dependent nonlinear spectral broadening and tunable offset filtering [7]. The bandwidth of the optical spectrum increases nonlinearly with increasing peak power of the input pulse injected into the nonlinear fiber. The pulse with high peak power will be broadened in the nonlinear fiber, while the signal with low peak power will not. With filtering at the broadened wavelength, the signal with low peak power will be suppressed while the signal with high peak power will be regenerated. The parameters of the optical filter are related to the performance of the regenerated signal.

To investigate the effects of the optical filter parameters on the regenerated signal from an AOT, an experimental test system for a supercontinuum-based AOT is set up as shown in Fig. 1. The input pulse is generated by a gain-switched laser with center wavelength of 1544.4 nm and repetition rate of 2.5 GHz, and the width of the output pulse is about 12 ps. The pulse is Gaussian-shaped in neither the time domain nor the spectral domain. The output signal is modulated by an intensity modulator (IM) driven by a 2^7-1 pseudorandom binary sequence (PRBS), and then injected to the AOT. The AOT consists of an erbium-doped fiber amplifier (EDFA), a variable optical attenuator (VOA), an 800-m HNLF span, and a wavelength-selective switch (WSS, Finisar WSS DWP-EK-AA). The modulated signal is amplified by the EDFA to induce nonlinear effects in HNLF. The maximum output power of the EDFA is 363.08 mW. The WSS has a flexible grid and a channel width resolution of 12.5 GHz. Thus the WSS can work as a bandpass filter with both center wavelength and bandwidth being tunable. One branch of the output signal from the AOT is tested by an optical spectral analyzer (OSA); the power of the other branch is controlled by a variable optical attenuator (VOA) followed by a photonic detector and oscilloscope.

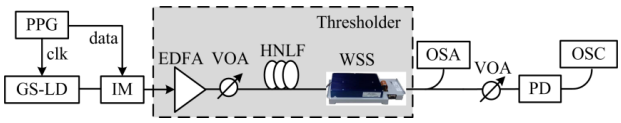

FIG. 1. Experimental setup of the test system for a supercontinuum-based AOT. PPG, programmable pulse generator; clk, clock; GS-LD, gain-switched laser; IM, intensity modulator; EDFA, erbium-doped fiber amplifier; VOA, variable optical attenuator; HNLF, highly nonlinear fiber; WSS, wavelength selective switch; OSA, optical spectral analyzer; PD, photonic detector; OSC, oscilloscope.

III. RESULTS AND DISCUSSION

First we measured the spectrum of the optical pulse after the HNLF. The spectra for different input powers of signal injected into the HNLF are shown in Figs. 2(a) and (b). As we can see in Fig. 2(a), the optical spectrum of the output signal keeps nearly stable when the input power is less than 6.31 mW. For signals in the input-power range of 6.31 to 15.85 mW, a new wavelength is observed in the range of 1545 to 1560 nm, because of the impact of weak self phase modulation (SPM) in the HNLF under these conditions. In Fig. 2(b) the bandwidth is broadened more, owing to the influence of SPM, and two peaks are observed on either side of the seeding. As the input power increases, the bandwidth increases, as does the difference between these two peaks; however, the amplitude noise does not broaden, as its peak power is too low to induce SPM. Thus the amplitude noise on the low level of a binary amplitude-modulated signal can be suppressed with offset filtering within the broadened wavelength range. When the input power is greater than 100 mW the spectrum becomes supercontinuum, due to the influence of four-wave mixing (FWM), self-steepening, stimulated Raman scattering (SRS), and other nonlinear effects. Since the input pulse is

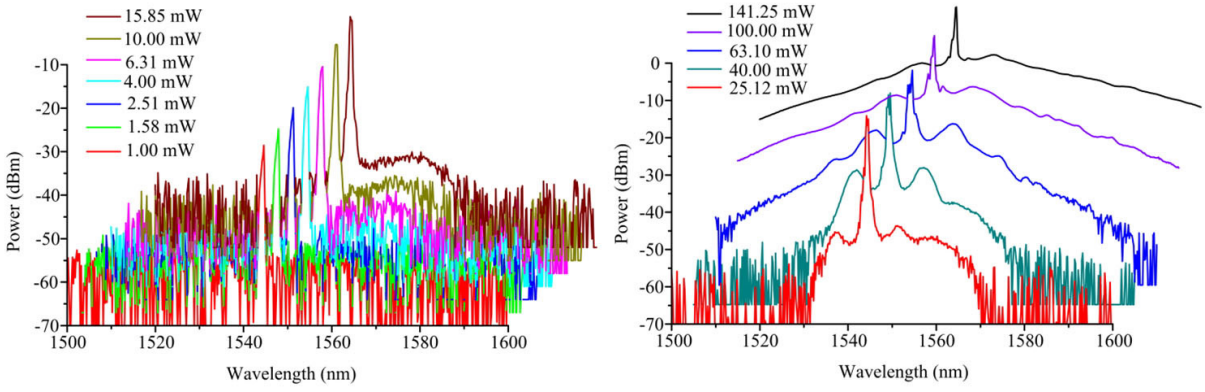

(a) (b)

FIG. 2. The spectra of the output signals after HNLF for input power (a) less than 20 mW, and (b) greater than 20 mW.

not Gaussian-shaped, its spectrum broadens asymmetrically. When the input power is further increased, the power at shorter wavelengths is saturated due to SRS, while the spectrum at longer wavelengths keeps increasing. Thus the amplitude noise on the high level of a binary amplitude-modulated signal can be suppressed in the shorter-wavelength range.

Figure 3 shows the 20-dB bandwidth of the output signal versus different input powers. As we can see, the bandwidth remains unchanged when the input power is below 30 mW. However, when the input power is over 40 mW, the optical spectrum of the output signal is broadened dramatically, and its 20-dB bandwidth increases linearly with increasing input power.

In the experiment, the power transfer function of the AOT is found by tuning the power of the signal injected to the HNLF, and measured under different filter parameters. The results measured at different center wavelengths with a 20-dB bandwidth of 3 nm are shown in Figs. 4(a) and (b). As we can see, most of the power transfer functions in Fig. 4(a) exhibit three linear regions, which include a flattened low-level region, a middle region, and a linear high-level region. The high-level region for center wavelengths below 1544.4 nm is relatively flat, compared to that for longer wavelengths, and as shown in Fig. 4(b), the high-level region for power transfer functions with center

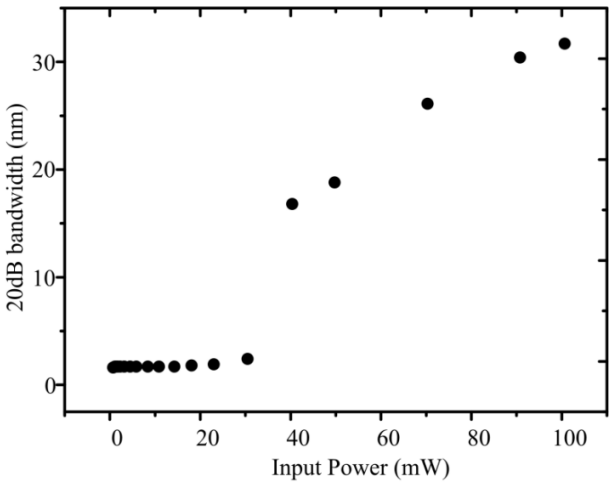

FIG. 3. The bandwidth of the output signal after HNLF versus the input power.

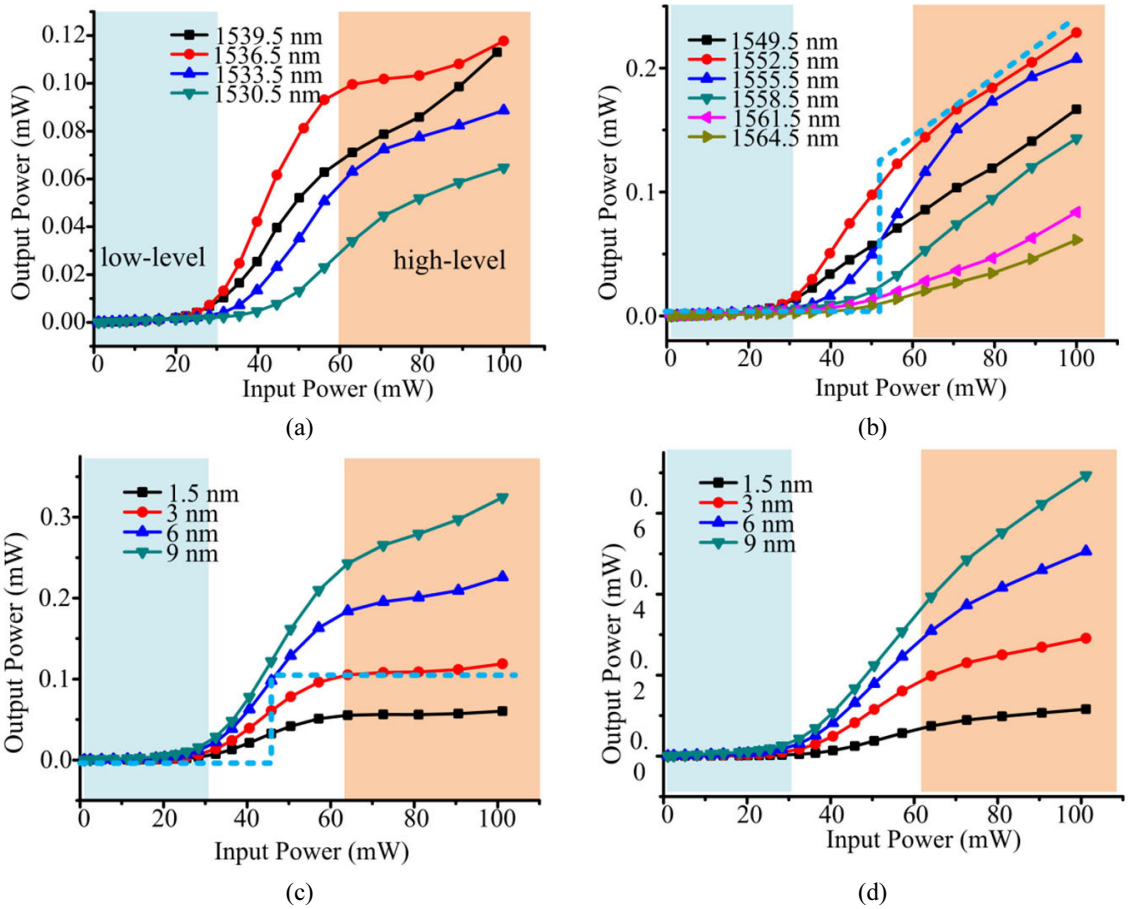

FIG. 4. The power transfer functions with (a) different filter center wavelengths less than 1544.4 nm, (b) different filter center wavelengths greater than 1544.4 nm, (c) different 20-dB bandwidths at a center wavelength of 1536.5 nm, and (d) different 20-dB bandwidths at a center wavelength of 1554 nm.

wavelength above 1544.4 nm is similar to the middle region. This is caused by asymmetric power increase on either side of the input signal, which is induced by SRS. These power transfer functions fit well with the measured optical spectrum in Fig. 2. The power transfer functions with center wavelengths of 1536.5, 1555.5, and 1552.5 nm each have a steep slope in the middle region. Figure 4(c) shows the measured results for different bandwidths at a center wavelength of 1536.5 nm, and Fig. 4(d) shows the results for 1554 nm. For the same center wavelength, wider bandwidth results in steeper middle and high-level regions of the function. For the functions at a center wavelength of 1536.5 nm, the high-level region is flattened for different bandwidths, because in the high-level region the energy in the wavelength range around 1536.5 nm is transferred to longer wavelengths due to the influence of SRS, but the power increases due to SPM. Therefore, the output power in the wavelength range around 1536.5 nm can be kept stable by the combined influences of SPM and SRS.

The power transmission function can be found by calculating the ratio of output power to input power. In a further discussion of the power transfer and transmission functions, we calculate the slope of each function at different levels. The slope for power functions with different center wavelengths and bandwidths are shown in Figs. 5(a) and (b). In the following discussion, "transfer slope" refers to the slope of the power transfer function, and "transmission slope" refers to the slope of the power transmission function. As shown in Fig. 5(a), the transfer slopes are similar to the transmission slopes in the low and middle levels. At the high level, the transfer slopes with longer center wavelength are larger than those with shorter. The ideal power function has a slope of 0 at high and low levels, but a steep slope in the middle. Thus, the power transfer functions with short center wavelengths show approximately ideal functional form, and the transfer function with a wavelength of 1536.5 nm, Fig. 5(c), shows a steplike form. According to the transmission slopes in Fig. 5(a), the transmission functions with short center wavelength and two long center wavelengths show approximately ideal forms. The transmission function with center wavelength of 1552.5 nm, Fig. 5(d), also shows a steplike form. Therefore, an AOT with short center wavelength can perform both thresholding and self-switching, while one with a long center wavelength only performs self-switching. For

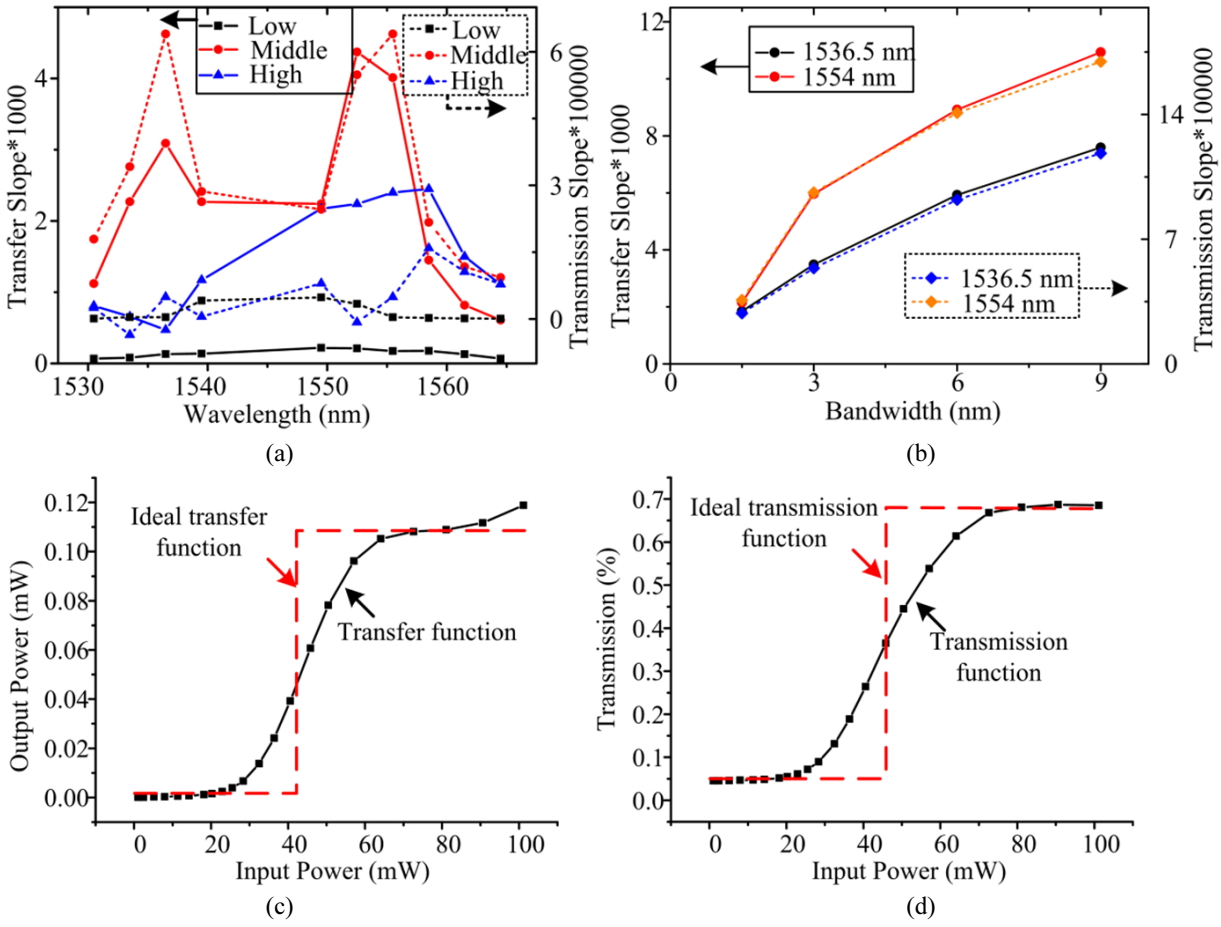

FIG. 5. The slope for (a) different center wavelengths and (b) different bandwidths, (c) the power transfer function, and (d) the power transmission function.

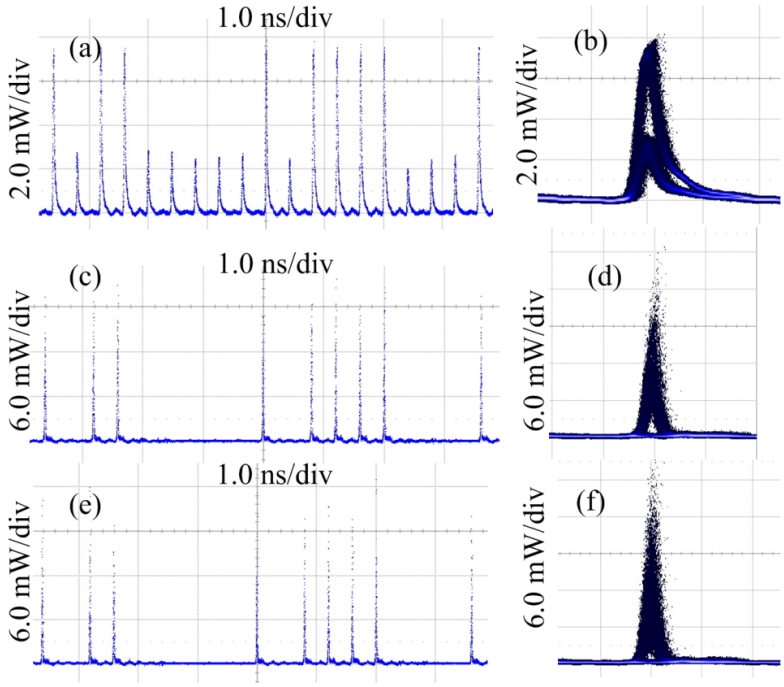

FIG. 6. The waveform (a) and eye diagram (b) before the AOT; the waveform (c) and eye diagram (d) after the AOT with short wavelength offset; the waveform (e) and eye diagrams (f) after AOT with long wavelength offset.

optical thresholding, the AOT can be used for all-optical logic[11] and analog-to-digital conversion[2]. For optical self-switching, the AOT can be used for noise suppression in optical stealth communication [12] and pulse-based amplitude-shift-keying systems. Figure 5(b) shows the transfer and transmission slopes with different bandwidths in the middle level. As we can see, both transfer and transmission slopes are proportional to bandwidth for each center wavelength. A steeper slope in the middle level represents better performance.

We also investigate the thresholding capacity by measuring the effect on a noisy signal. Figures 6(a) and (b) show the waveform and eye diagram of the input noisy signal respectively. The noisy signal with 2^7-1 PRBS bit pattern is generated by controlling the bias of the IM to introduce amplitude noise into the low level. Figures 6(c) and (d) show the waveform and eye diagram of the signal output from the AOT with the same parameters as in Fig. 5(c), while Figs. 6(e) and (f) show them with same parameters as in Fig. 5(d). Concerning the waveform, the AOT can suppress noise effectively with either parameter set. In terms of the eye diagrams, the AOT with the same parameters as in Fig. 5(c) gives better performance. To quantitatively analyze the difference between the two eye diagrams, their eye-opening penalties [13] are calculated. Figure 6(f) has about 5 dB more eye-opening penalty than Fig. 6(d). This is because the filter parameters affect the performance of the AOT, and the AOT with short center wavelength has a better power transfer function. The result matches the analysis results for the power functions.

IV. CONCLUSION

The effects of filter parameters on the performance of a supercontinuum-based AOT are demonstrated. Based on the AOT test system, the broadened spectra are measured, and it shows nonlinear increase of bandwidth with increasing input power. By tuning the filter parameters of the AOT, its power transfer and transmission functions can be tailored. The results show that an AOT with short center wavelength has a better power function than with a long one, and the performance of the AOT is proportional to the bandwidth. By tuning the filter parameters, the AOT has a steplike power transfer function for optical thresholding and a steplike power transmission function for optical self-switching. Amplitude noise can be effectively suppressed by the AOT, and the results match the analysis results for the power function.

ACKNOWLEDGMENT

The work was supported in part by the National Natural Science Foundation of China under grant No. 61475193 and No. 61174199, and the Jiangsu Province Science Foundation under grant No. BK20140069.

REFERENCES

1. F. Ramos, E. Kehayas, J. M. Martinez, R. Clavero, J.

Marti, L. Stampoulidis, D. Tsiokos, H. Avramopoulos, J. Zhang, P. V. Holm-Nielsen, N. Chi, P. Jeppesen, N. Yan, I. Tafur, Monroy, A. M. J. Koonen, M. T. Hill, Y. Liu, H. J. S. Dorren, R. Van Caenegem, D. Colle, M. Pickavet, and B. Riposati, "IST-LASAGNE: towards all-optical label swapping employing optical logic gates and optical flip-flops," IEEE J. Lightwave Technol. **23**, 2993-3011 (2005).

2. Y. Miyoshi, S. Takagi, S. Namiki, and K.-I. Kitayama, "Multiperiod PM-NOLM with dynamic counter-propagating effects compensation for 5-bit all-optical analog-to-digital conversion and its performance evaluations," IEEE J. Lightwave Technol. **28**, 415-422 (2010).
3. K. Kravtsov, P. R. Prucnal, and M. M. Bubnov, "Simple nonlinear interferometer-based all-optical thresholder and its applications for optical CDMA," Opt. Express **15**, 13114-13122 (2007).
4. M. A. Nahmias, B. J. Shastri, A. N. Tait, M. Eder, N. Rafidi, Y. Tian, and P. R. Prucnal, "Normalized pulsed energy thresholding in a nonlinear optical loop mirror," Appl. Opt. **54**, 3218-3224 (2015).
5. N. S. Rafidi, K. S. Kravtsov, Y. Tian, M. P. Fok, M. A. Nahmias, A. N. Tait, and P. R. Prucnal, "Power transfer function tailoring in a highly Ge-Doped nonlinear interferometer-based all-optical thresholder using offset-spectral filtering," IEEE Photon. Journal **4**, 528-534 (2012).
6. C. Guo, X. Hong, and S. He, "Elimination of multiple access interference in ultrashort pulse OCDMA through nonlinear polarization rotation," IEEE Photon. Technol. Lett. **21**, 1484-1486 (2009).
7. P. V. Mamyshev, "All optical data regeneration on self-phase modulation effect," in *Proc. 24th European Conference on Optical Communication* (Madrid, Spain, Sep. 1998), pp. 475-476.
8. X. Wang, T. Hamanaka, N. Wada, and K. Kitayama, "Dispersion-flattened-fiber based optical thresholder for multiple-access-interference suppression in OCDMA system," Opt. Express **13**, 5499-5505 (2005).
9. Y. Chen, R. Wang, T. Pu, P. Xiang, T. Fang, F. Zhen, and J. Zheng, "Effect of filter parameters on enhanced performance of highly nonlinear fiber-based all optical thresholding," Opt. Eng. **52**, 045002 (2013).
10. E. Ciaramella, "Wavelength conversion and all-optical regeneration: achievements and open issues," IEEE J. Lightwave Technol. **30**, 415–422 (2012).
11. S. Ma, Z. Chen, H. Sun, and N. K. Dutta, "High speed all optical logic gates based on quantum dot semiconductor optical amplifiers," Opt. Express **18**, 6417-6422 (2010).
12. H. Zhu, R. Wang, T. Pu, T. Fang, P. Xiang, J. Zheng, and D. Chen, "Optical stealth transmission based on super-continuum generation in highly nonlinear fiber over WDM network," Opt. Lett. **40**, 2561-2563 (2015).
13. X. Chen, P. R. Horche, and A. M. Minguez, "Analysis of signal impairment and crosstalk penalty induced by different types of optical filters in 100 Gbps PM-DQPSK based systems," in *Proc. 2014 19th European Conference on Networks and Optical Communications* (Milano, Italy, Jun., 2014), pp. 35-40.